

Hyperosmolality Inhibits Exocytosis in Sea Urchin Eggs by Formation of a Granule-Free Zone and Arrest of Pore Widening

Carrie J. Merkle and Douglas E. Chandler

Department of Zoology, Arizona State University, Tempe, Arizona 85287

Summary. Hyperosmolality is known to inhibit membrane fusion during exocytosis. In this study cortical granule exocytosis in sea urchin eggs is used as a model system to determine at what step this inhibition occurs. *Strongylocentrotus purpuratus* eggs were incubated in hyperosmotic seawater (Na_2SO_4 , sucrose or sodium HEPES used as osmoticants), the eggs activated with $20 \mu\text{M}$ A23187 to trigger exocytosis, and then quick frozen or chemically fixed for electron microscopy. Thin sections and freeze-fracture replicas show that at high osmolality (2.31 osmol/kg), there is a decrease in cortical granule size, a 90% reduction in granule-plasma membrane fusion, and formation of a granule-free zone between the plasma membrane and cortical granules. This zone averages $0.64 \mu\text{m}$ in thickness and prevents the majority of granules from docking at the plasma membrane. The remaining granules (~10%) exhibit early stages of fusion which appear to have been stabilized; the matrix of these granules remains intact. We conclude that exocytosis is blocked by two separate mechanisms. First, the granule-free zone prevents granule-plasma membrane contact required for fusion. Second, in cases where fusion does occur, opening of the pocket and dispersal of the granule contents are slowed in hyperosmotic media.

Key Words membrane fusion · exocytosis · hyperosmolality · cortex · sea urchin egg · freeze fracture

Introduction

Sea urchin eggs, upon activation with either sperm or calcium ionophore, undergo cortical granule exocytosis. Osmotic forces are definitely involved in this process; however, it is not known what the full role of water movement is and specifically when in exocytosis it occurs.

Hyperosmolality inhibits exocytosis in sea urchin eggs (Zimmerberg & Whitaker, 1985) and other cells including adrenal chromaffin cells (Hampton & Holz, 1983; Pollard et al., 1984), neutrophils (Kazilek, Merkle & Chandler, 1988), and platelets (Pollard et al., 1977). It is thought that the lowered water activity in the extracellular space slows or prevents swelling of secretory vesicles, though it is not clear when swelling occurs (Finkelstein, Zim-

merberg & Cohen, 1986; Holz, 1986). One possibility is that swelling is a prerequisite for membrane fusion. Observations in model systems show that artificial vesicles fuse to planar membranes when an osmotic gradient is created between the vesicle-containing compartment and the *trans* compartment (Cohen, Zimmerberg & Finkelstein, 1980; Cohen et al., 1984). Furthermore, in cortical fragments of sea urchin eggs, calcium is thought to induce swelling of granules prior to exocytosis (Zimmerberg, Sardet & Epel, 1985; Zimmerberg & Whitaker, 1985).

A second possibility is that water movement and granule swelling occur just after granule-plasma membrane fusion. In mast cells, for example, it appears that membrane fusion actually precedes granule swelling as indicated by a correlation of electrophysiological and microscopic data (Breckenridge & Almers, 1987; Zimmerberg et al., 1987). Furthermore, water and ion movement appear to be important for widening of the exocytic pore and dispersal of granule contents in several systems. Cortical granule content dispersal in sea urchin eggs can be blocked by high molecular weight polymers (Whitaker & Zimmerberg, 1987; Chandler, Whitaker & Zimmerberg, 1989), while calcium ions are required for proper discharge of trichocysts in *Paramecium* (Plattner, Reichel & Matt, 1977; Bilinski, Plattner & Matt, 1981; Gilligan & Satir, 1983).

Hyperosmolality may also affect other aspects of exocytosis unrelated to granule swelling. In neutrophils, hyperosmolality inhibits components of the intracellular calcium signal responsible for triggering exocytosis (Kazilek et al., 1988). Hyperosmolality also activates the Na^+/H^+ antiport resulting in cytoplasmic alkalization in lymphocytes (Grinstein et al., 1985) and erythrocytes (Parker & Castranova, 1984). Since a rise in intracellular pH is thought to induce actin polymerization in sea urchin eggs (Begg & Rebhun, 1979), it is reasonable to ex-

pect that hyperosmolality might affect cytoskeletal elements involved in positioning the granules within the egg cortex. The mechanism of osmotic inhibition, then, could be more complex than mere prevention of swelling.

Although hyperosmotic effects on exocytosis are well known, it is surprising that there are few, if any, studies in the literature that actually document such effects on granule-plasma membrane fusion at the EM level. In this report we determine the ultrastructural basis for hyperosmotic inhibition of exocytosis in the sea urchin egg cortex. In both quick-frozen and chemically fixed eggs, the majority of cortical granules become separated from the plasma membrane by an essentially organelle-free zone formed by extensive reorganization of the cortical cytoskeleton. A small portion of granules remain docked, however, and in activated cells these allow us to visualize early stages of membrane fusion that have been arrested by hyperosmotic conditions.

Materials and Methods

Pacific sea urchins, *Strongylocentrotus purpuratus*, were obtained commercially (Marinus, Irvine, CA) and maintained at 11°C in artificial seawater ("Tropicmarin," Dr. Biener, GMBH, West Germany). Release of gametes was stimulated by injecting 0.5 M KCl into the body cavity. Eggs were collected in seawater at 10°C, passed twice through a 150- μ m mesh nylon cloth, acid dejellied at pH 5.0 for 1½ min, washed twice in seawater, and kept at 10°C until use. Sperm were collected "dry," kept at 5°C, and diluted 1:1000 with seawater 5 min before use to fertilize eggs. For our experiments, we used batches of eggs in which 95% or greater showed elevation of the fertilization envelope (FE) upon fertilization.

All experiments were performed at 15°C in artificial seawater (ASW) containing (in mM/liter): NaCl, 484; KCl, 10; MgCl₂, 27; MgSO₄, 29; CaCl₂, 11; NaHCO₃, 2.4; pH 8.1; 1.07 osmol/kg. Hyperosmotic seawater (HSW) was prepared by addition of either Na₂SO₄, sucrose or sodium HEPES to ASW. Osmolality was measured using a Wescor vapor pressure osmometer, which had been calibrated using standard NaCl solutions.

All experiments followed a standard protocol. A 0.1-ml aliquot of packed eggs was added to 0.9 ml ASW or HSW, preincubated 5 min, then activated by addition of calcium ionophore A23187 (final concentration 20 μ M). A23187 was added from a DMSO stock; final concentration was 1%, which did not affect exocytosis or cortex morphology (Whitaker & Zimmerberg, 1987). Five min after activation, eggs were either quick frozen or chemically fixed for EM, or examined for FE elevation by light microscopy. Egg viability was not affected by hyperosmotic treatment since the fertilization rate in ASW after a 10-min incubation at 2.31 osmol/kg was greater than 95%.

Samples for freeze fracture or thin sectioning were chemically fixed by addition of an equal volume of 4% glutaraldehyde in ASW or HSW identical to that used for incubation. Fixation was carried out at room temperature for 1 hr, then continued overnight at 5°C. The eggs for freeze fracture were washed, suspended in 25% glycerol/75% ASW or HSW for 30 min, and pelleted by a brief (<1 sec) submaximal velocity spin in a microfuge.

A drop of pelleted eggs was then placed on gold-alloy specimen carriers and frozen in melting Freon. Samples were fractured at -110°C in a Balzers 400 freeze-etch unit (Balzers AG, Balzers, Liechtenstein), allowed to etch 15 sec, and replicated with platinum-carbon from an electron beam gun mounted at a 45° angle. Replicas were cleaned overnight in bleach, rinsed by floating on distilled water, placed on formvar-coated carbon-stabilized copper grids, and visualized in a Philips 201 EM at 80 kV.

Eggs for thin sectioning were post-fixed in 1% osmium in seawater for 1.5 hr, rapidly dehydrated in a graded alcohol series, and embedded in Araldite 502. Silver sections were stained with 2% uranyl acetate and Reynolds' lead citrate (Reynolds, 1963) and viewed as above.

Samples to be quick frozen were pelleted by a brief (<1 sec) submaximal velocity spin in a microfuge. After removal of the supernatant, an 8- μ l aliquot was placed on an aluminum planchet and the sample was quick frozen on a liquid helium-cooled copper block in the machine designed by Heuser et al. (1979). Samples were stored in liquid nitrogen and fractured directly on the planchet using the procedure described above.

Measurements of cortical granule length and width and cortical granule-plasma membrane separation were made from negatives of freeze-fracture replicas. Negative magnification was determined by calibration with a diffraction grating replica. Measurements were restricted to granules that had been fractured in a manner leaving a complete ovoid view of the granule membrane. A parameter related to cross-sectional area of the cortical granules, k , was determined using the formula for the area of an ellipse:

$$k = ab\pi$$

where $a = \frac{1}{2}$ granule length and $b = \frac{1}{2}$ granule width. Validity of this method was determined by comparing actual cross-sectional area with k for 20 cortical granules; cross-sectional area and k were highly correlated ($r = 0.996$).

Results

Activation of *S. purpuratus* eggs with calcium ionophore in ASW (1.07 osmol/kg) results in nearly 100% FE elevation within 5 min (square, Fig. 1). In contrast, eggs activated in Na₂SO₄-HSW (ASW containing Na₂SO₄ to increase osmolality) exhibit a progressive inhibition in FE elevation as the medium osmolality is increased (triangles, Fig. 1); inhibition becomes evident at an osmolality of 1.48 osmol/kg and is complete by 2.31 osmol/kg. Similar results are obtained for the other osmoticants including sucrose (circles, Fig. 1) and sodium HEPES (*data not shown*) and in *Lytechinus pictus* eggs (Zimmerberg & Whitaker, 1985). Inhibition of FE elevation is not due to the osmotic properties of the vitelline layer or the FE as these are permeable to water and ions.

Examination by light microscopy shows that as osmolality of the medium is increased, there is a progressive crenated appearance to the eggs (Fig. 2B and C) in comparison to eggs in ASW (Fig. 2A).

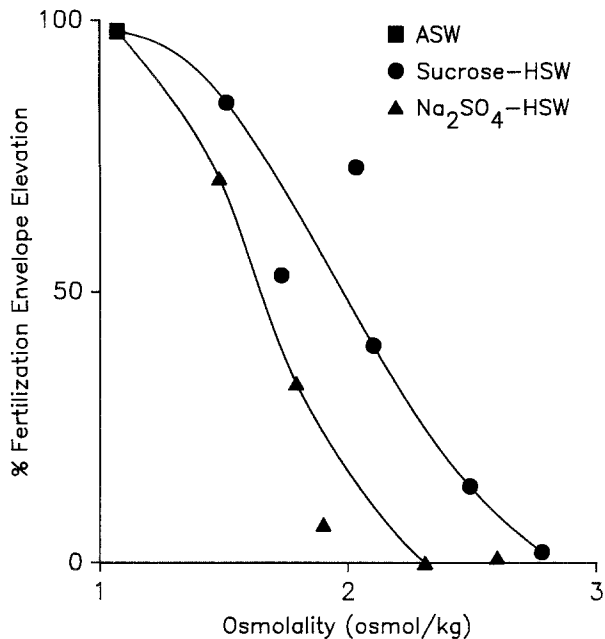


Fig. 1. Inhibition of FE elevation in *S. purpuratus* eggs incubated in HSW. Eggs were preincubated in Na₂SO₄-HSW (▲) or sucrose-HSW (●) for 5 min, then 20 μM A23187 was added. Eggs were scored for FE elevation using light microscopy 5 min later

Eggs treated with A23187 in Na₂SO₄-HSW at osmolalities that result in partial inhibition (1.79 and 1.90 osmol/kg) exhibit localized bubbles of FE elevation (Fig. 2B) suggesting incomplete cortical granule exocytosis; at higher osmolalities FE elevation is absent (Fig. 2C).

At the ultrastructural level, the cortex of *S. purpuratus* eggs displays a single layer of ovoid cortical granules just under the plasma membrane (Fig. 3A). In thin sections, cortical granules exhibit a characteristic lamellar structure (Fig. 3B). Five min after addition of A23187, cortical granule exocytosis is complete, exocytic pockets are gone, and the contents of the cortical granules are dispersed in the extracellular space (Fig. 3C). As seen in freeze-fracture replicas, the surface of the activated egg is studded with microvilli having finger-like extensions from broad bases (Fig. 3D).

Eggs incubated in Na₂SO₄-HSW (2.31 osmol/kg) exhibit a radically different architecture (Fig. 4A). Cortical granules have separated from the plasma membrane resulting in a granule-free zone (GFZ). The GFZ is organelle-free except for fragments of cortical endoplasmic reticulum (arrow,

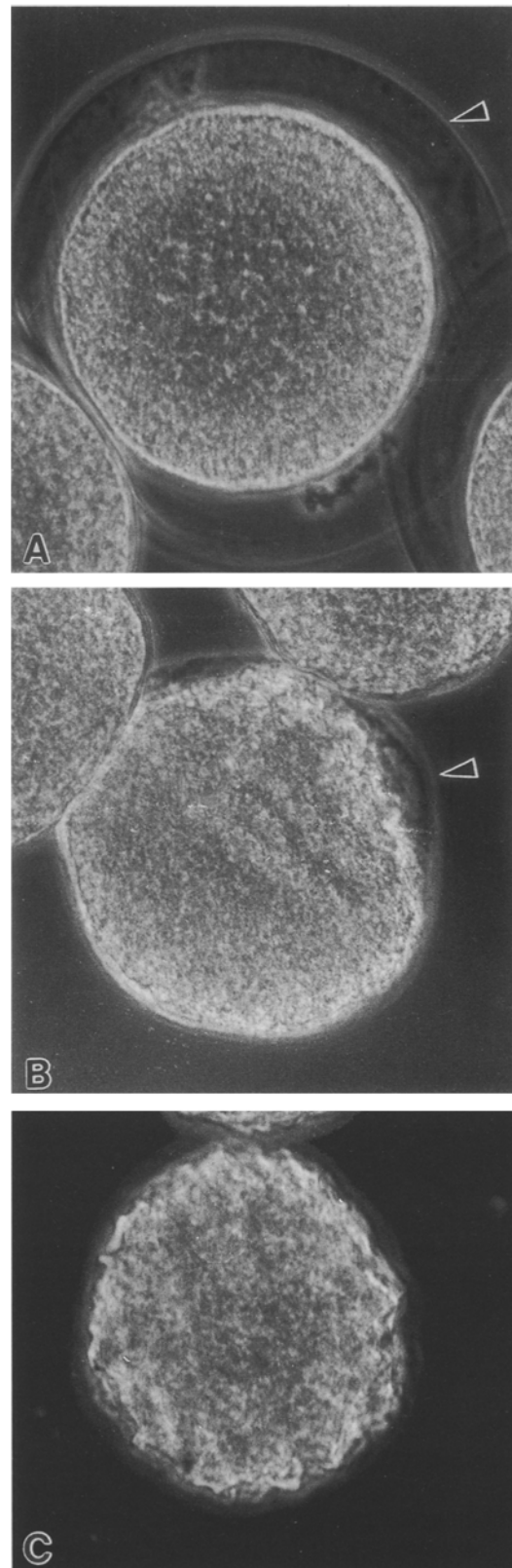


Fig. 2. Phase-contrast micrographs of eggs activated with A23187 in ASW or Na₂SO₄-HSW. (A) Eggs activated in ASW (1.07 osmol/kg) exhibit fully elevated FEs (arrow). (B) Eggs activated in Na₂SO₄-HSW (1.90 osmol/kg). FE elevation is absent or

partial (arrow). (C) Eggs activated in Na₂SO₄-HSW (2.31 osmol/kg) show no FE elevation. Specimens were fixed in 2% glutaraldehyde in ASW or HSW identical to that used in preincubation. 550×

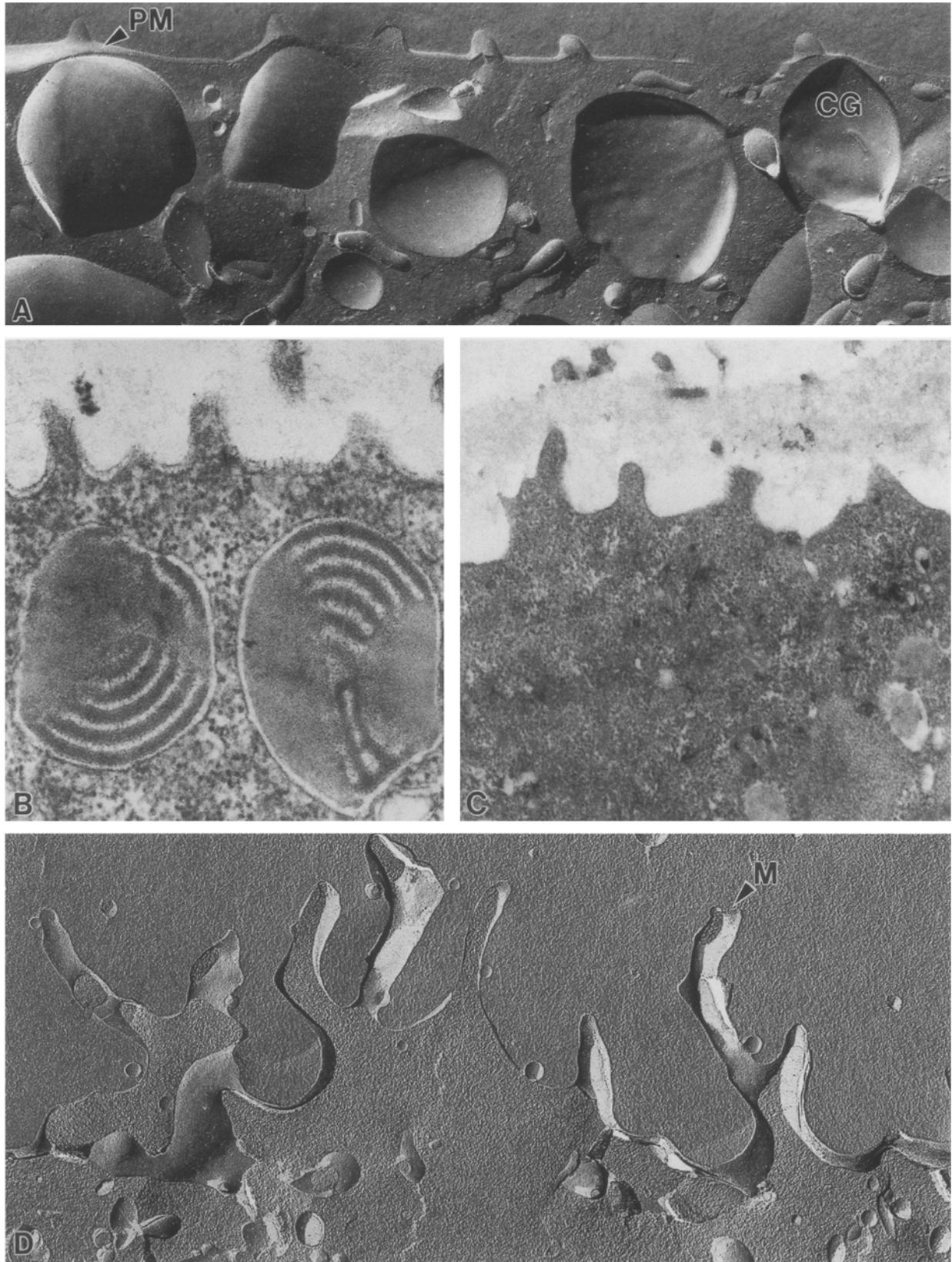


Fig. 3. Electron micrographs of the egg cortex in ASW (1.07 osmol/kg) before (A, B) and after (C, D) activation. (A) Freeze-fracture replica of quick-frozen egg reveals that cortical granules (CG) lie in a single layer just under the plasma membrane (PM). 34,000 \times . (B) Granules have a characteristic internal lamellar structure. 61,200 \times . (C) Five min after activation with A23187, exocytosis is complete and the granule contents have dispersed in the egg. 30,000 \times . (D) Freeze-fracture replica of fixed eggs demonstrates the presence of long finger-like microvilli 5 min after activation. 34,000 \times

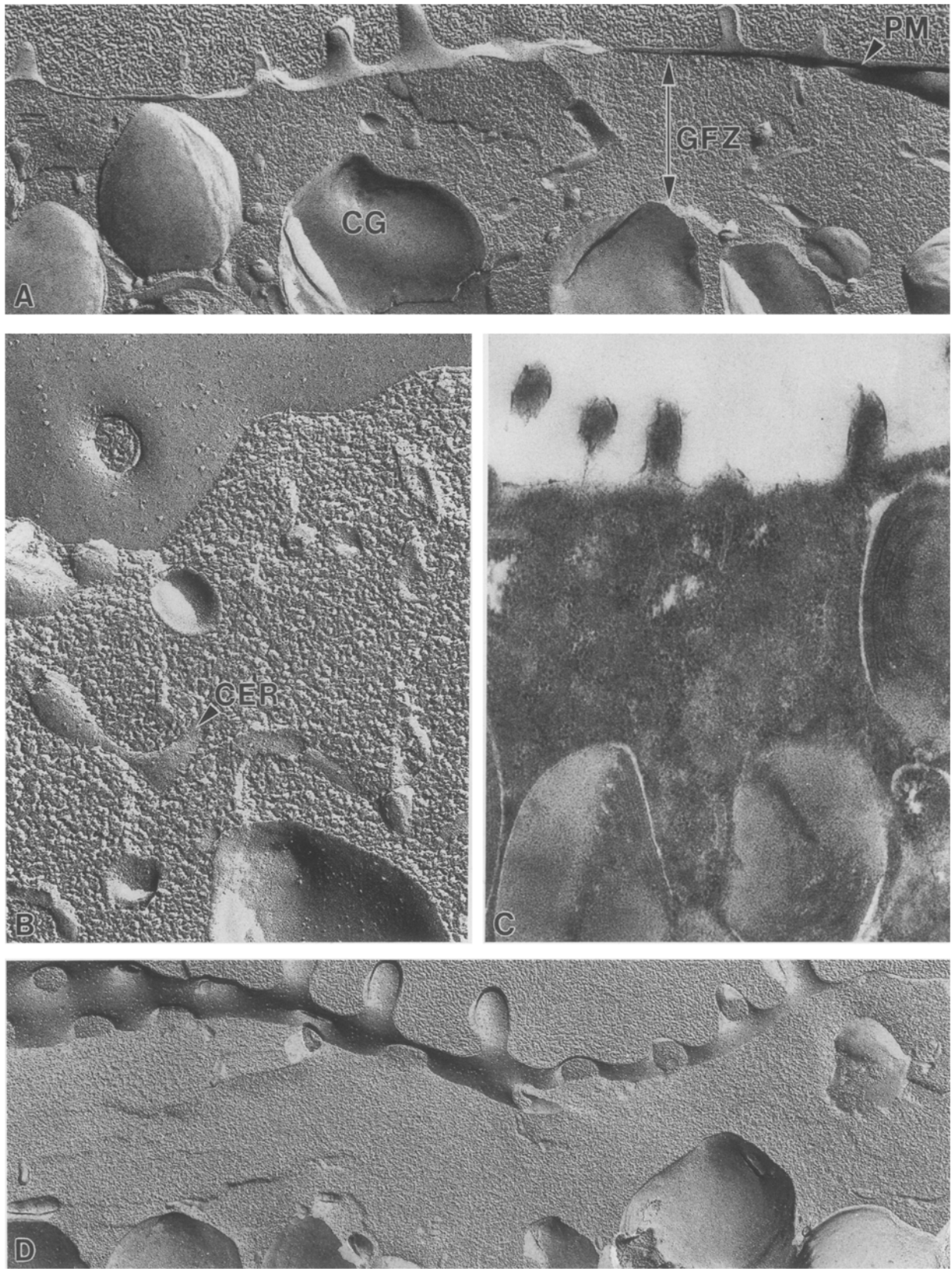


Fig. 4. The egg cortex before (A–C) and after (D) activation in Na_2SO_4 -HSW (2.31 osmol/kg). (A) Freeze-fracture replica of an egg quick frozen after a 10-min incubation in Na_2SO_4 -HSW. Most cortical granules (CG) are widely separated from the plasma membrane (PM) creating a granule-free zone (GFZ). Occasional granules remain docked. (B) Cortical endoplasmic reticulum (CER) is the only organelle in the GFZ. 80,600 \times . (C) Thin sections of eggs fixed in Na_2SO_4 -HSW show that the GFZ is filled with cytoskeletal elements. 54,100 \times . (D) The GFZ in an egg preincubated in Na_2SO_4 -HSW (2.31 osmol/kg), activated 5 min later with 20 μM A23187, and fixed 5 min after ionophore addition. Granules are still well separated from the plasma membrane and granule-plasma membrane fusion is absent. 34,000 \times .

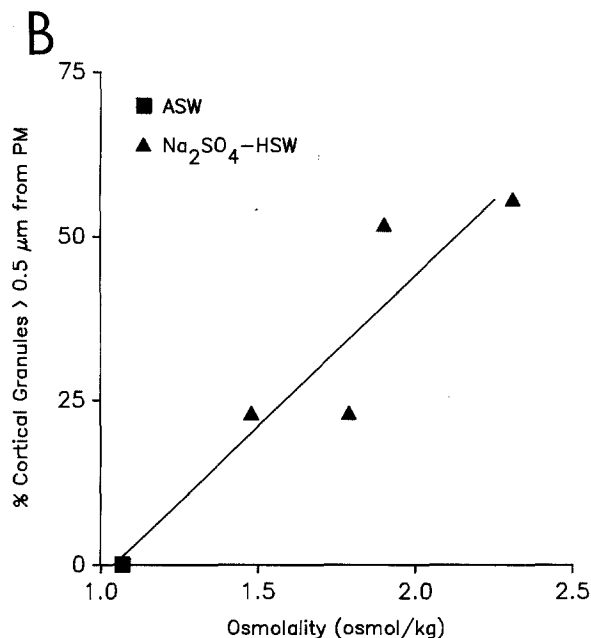
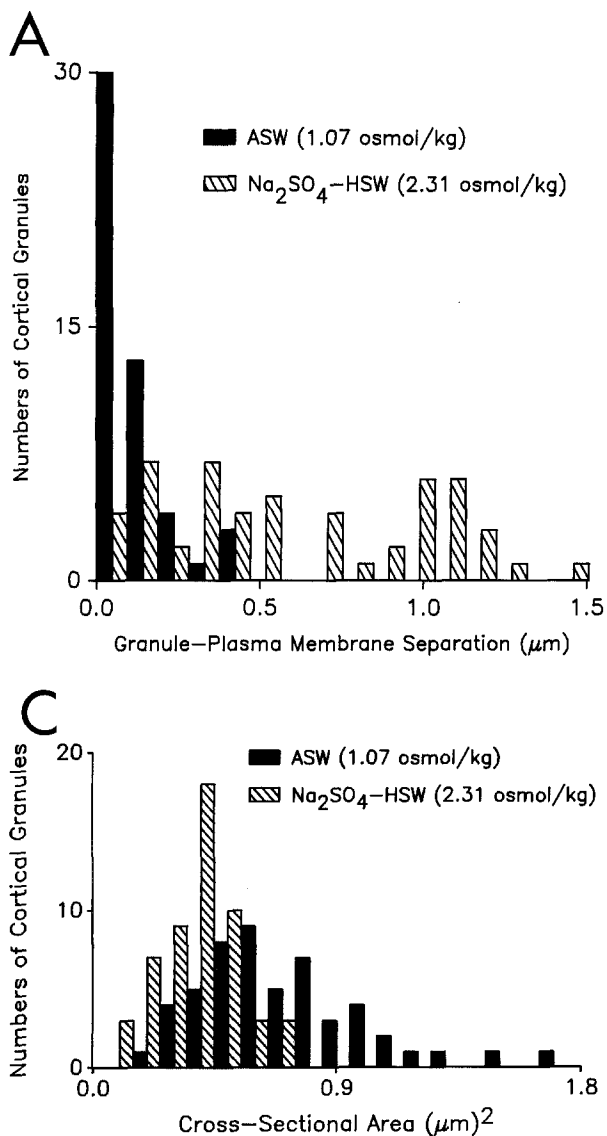


Fig. 5. (A) Histogram of cortical granule-plasma membrane separation. The closest approach between individual cortical granules and the plasma membrane was measured on negatives of eggs that had been incubated in either ASW (1.07 osmol/kg) (solid bars) or in Na_2SO_4 -HSW (2.31 osmol/kg) for 10 min (hatched bars). Samples were fixed in 2% glutaraldehyde, freeze fractured, and replicas photographed at 5,000 \times . (B) Percentage of cortical granules greater than 0.5 μm from the plasma membrane as a function of seawater osmolality. Measurements were made as in Fig. 5A. Osmolality of the seawater was increased by adding Na_2SO_4 . (C) Histogram distribution for cross-sectional area of cortical granules of eggs incubated in ASW (1.07 osmol/kg) (solid bars) or in Na_2SO_4 -HSW (2.31 osmol/kg) (hatched bars). Measurements were made as described in Fig. 5A

Fig. 4B). In addition, cortical granules have a furrowed appearance and appear shrunken in comparison to their ovoid shape in ASW. Thin sections (Fig. 4C) show that the GFZ appears to contain cytoskeletal filaments, possibly polymerized actin, but this needs to be verified.

Eggs activated in Na_2SO_4 -HSW (2.31 osmol/kg) show almost no signs of granule fusion after addition of A23187. Both replicas (Fig. 4D) and thin sections (Fig. 6A) demonstrate that the GFZ is maintained during activation and that cortical granules and the plasma membrane are unable to fuse because of their separation. These results were not dependent on fixative osmolality, since formation of the GFZ and lack of granule fusion was seen in both quick-frozen and glutaraldehyde-fixed samples.

Formation of the GFZ was further characterized by quantitative measurements on EM nega-

tives. A histogram of the distances separating individual cortical granules from the plasma membrane shows that normally, in seawater, most granules lie within 0.1 μm of the cell surface (solid bars, Fig. 5A). In contrast, formation of the GFZ in Na_2SO_4 -HSW (2.31 osmol/kg) is accompanied by a granule-plasma membrane separation that has a mean of $0.64 \pm 0.06 \mu\text{m}$ ($\pm\text{SEM}$, $n = 52$) and can be as great as 1.5 μm (hatched bars, Fig. 5A). Furthermore, as the osmolality of the Na_2SO_4 -HSW is increased, the percentage of cortical granules separated by more than 0.5 μm from the plasma membrane increases progressively in a dose-dependent manner (Fig. 5B). In addition to formation of the GFZ, increased osmolality of the Na_2SO_4 -HSW is accompanied by granule shrinkage as indicated by a shift in the cross-sectional areas of individual cortical granules toward smaller values (Fig. 5C). The difference be-

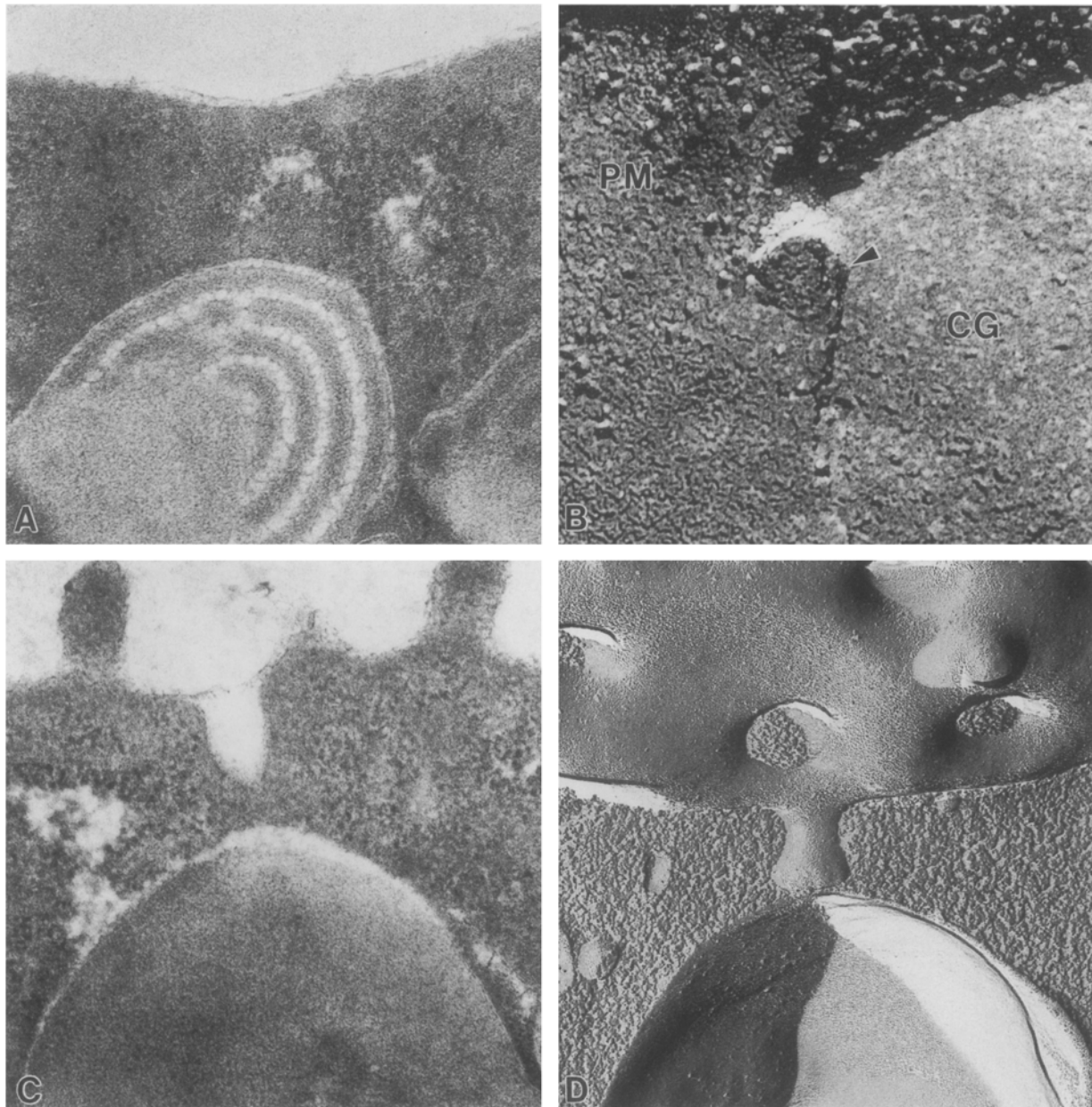


Fig. 6. Cortical granule-plasma membrane interactions in eggs preincubated in $\text{Na}_2\text{SO}_4\text{-HSW}$ (2.31 osmol/kg) for 5 min, and activated with $20 \mu\text{M}$ A23187. (A) Most granules remain separated from the plasma membrane by a GFZ filled with cytoskeletal elements. $80,000\times$. (B) The few cortical granules (CG) that remain in close contact with the plasma membrane (PM) fuse forming pores as small as 50 nm (arrow). $265,000\times$. (C, D) Frequently there are instances in which the plasma membrane dips toward the granule. (C) $90,000\times$. (D) $77,500\times$. Specimens were fixed with 2% glutaraldehyde 5 min after activation

tween the mean cross-sectional area of granules from the two samples is statistically significant ($P < 0.001$, Student's *t* test).

Although GFZ formation blocks fusion of 89% of the cortical granules in eggs activated in 0.6 M $\text{Na}_2\text{SO}_4\text{-HSW}$ (2.31 osmol/kg) (312 cortical granules counted in three experiments), about 10% of the cortical granules do fuse, presumably those that remain docked near the plasma membrane. Granule-

plasma membrane fusion, when it does occur, is arrested at very early stages. In some cases, pores as small as 50 nm in diameter are seen joining the granule and plasma membranes (Fig. 6B). Prior to fusion the plasma membrane appears to dip toward the granule bringing the two membranes into close proximity (Fig. 6C and D). Membrane fusion occurs, and the granule is joined to the plasma membrane by a "narrow-necked" pore (Fig. 7A and B),

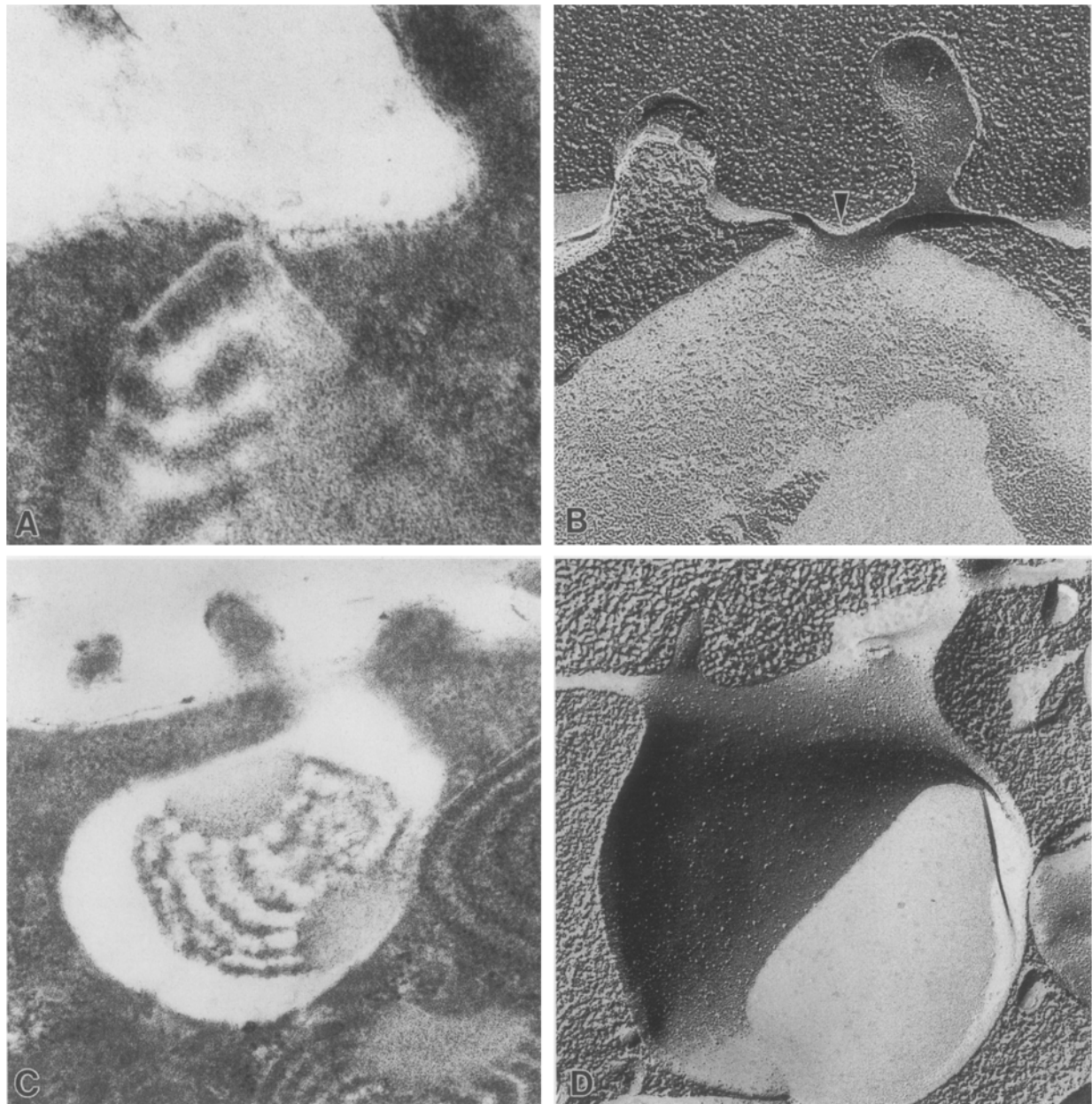


Fig. 7. Arrest of pore widening in Na_2SO_4 -HSW. Eggs were activated with A23187 and fixed 5 min later as described in Fig. 6. (A, B) The formation of a "narrow-necked" pore (arrow) between the plasma membrane and cortical granule is captured under hyperosmotic conditions. (A) 158,000 \times . (B) 99,200 \times . (C, D) Hyperosmotic media arrest widening of the exocytic pocket and block dispersal of the contents of the granule. (C) 74,400 \times . (D) 55,800 \times

which widens to produce an omega-configured exocytic pocket (Fig. 7C and D). Invariably, the granule contents have failed to disperse. In this sample, in fact, virtually all granules that exhibited an arrest of granule-plasma membrane fusion ($\sim 10\%$) also had intact lamellar structures. This suggests that pore widening and discharge of granule contents are linked and both are inhibited by hyperosmotic media.

Discussion

An important finding in this study, entirely unanticipated, is that hyperosmolality alters the architecture in the cortex of *S. purpuratus* eggs creating a GFZ separating the majority of the cortical granules from the plasma membrane. In ASW, most granules are within $0.1 \mu\text{m}$ of the plasma membrane, where as in Na_2SO_4 -HSW (2.31 osmol/kg) the majority of

granules are at least 0.5 μm from the plasma membrane. Separation increases as osmolality is increased and the GFZ formed is seen in both quick-frozen and chemically fixed eggs suggesting that it is not a fixation artifact. Granule-plasma membrane separation prevents granule fusion that would normally be complete at 5 min after A23187 activation. The cortical granules are simply too far from the plasma membrane to fuse.

Formation of the GFZ was not anticipated because previous studies of hyperosmolality effects on secretion were limited to enzyme release measurement and light microscopic observations. In the absence of ultrastructural data, these studies attributed inhibition to a defect in membrane fusion—the absence of granule swelling prior to fusion. It is now clear that the major defect is in cytoskeletal organization and not in membrane fusion. It appears that the cortex becomes filled with cytoskeletal filaments, which NBD-phalloidin shows to be filamentous actin (C.J. Merkle & D.E. Chandler, *unpublished observation*). Evidently extensive reorganization of cortical actin occurs. Actin is normally located in short filaments in a honeycomb arrangement within each microvillus; a few longer bundles are restricted to areas just beneath the plasma membrane (Henson & Begg, 1988). In addition, there is a large pool of G-actin in unactivated eggs which is thought to serve as a reservoir for actin polymerization just after fertilization. Polymerization results in formation of a dense network of actin filaments in the embryo cortex (Mabuchi & Spudich, 1980).

Why might actin polymerization occur in response to increases in osmolality? One possibility is that hyperosmolality causes an intracellular pH change. Many cells respond to hyperosmotic conditions by activation of a Na^+/H^+ exchanger (Parker & Castranova, 1984; Grinstein et al., 1985), which moves H^+ out of the cell. Sea urchin eggs, in fact, have such an antiport, which alkalinizes the cytoplasm just after fertilization (Payan, Girard & Ciapa, 1983). This pH change at fertilization is known to promote cortical actin polymerization (Begg & Rebhun, 1979), and therefore it is quite possible that hyperosmolality induces actin polymerization by a pH signal in much the same manner.

Despite formation of the GFZ, about 10% of the cortical granules remain docked at the plasma membrane. Upon activation these granules fuse with the plasma membrane but fusion is arrested at a very early stage in hyperosmotic media. From examination of these early stages, it appears that fusion can be divided into three steps. First, the plasma membrane dips toward the cortical granule to bring these

membranes into close contact. Second, a small, "narrow-necked" pore forms joining the cortical granule to the plasma membrane. Third, the pore widens to form an omega-shaped exocytic pocket. These steps are consistent with findings showing formation of a small pore as an initial step in exocytosis in mast cells and neutrophils (Chandler & Heuser, 1980; Chandler, Bennett & Gomperts, 1983) and of small indentations in the plasma membrane toward cortical granules in sea urchin eggs (Zimmerberg et al., 1985).

In sea urchin eggs, hyperosmolality inhibits these early steps of fusion and, in particular, widening of the exocytic pocket. The granule cores remain intact even in cortical granules in which obvious granule-plasma membrane fusion has occurred (Fig. 7A and C). Lack of granule content dispersal, i.e., the presence of intact lamellar structures, is apparent in virtually all fused cortical granules. This demonstrates that small molecular weight osmoticants at sufficiently high osmolalities (>2.31 osmol/kg) can arrest exocytosis immediately after pore formation and before the pore has widened. Arrest by Na_2SO_4 and sucrose contrasts to that seen with high molecular weight dextrans (Whitaker & Zimmerberg, 1987; Chandler et al., 1989). Dextrans also inhibit granule matrix dispersal but pore growth takes place normally and exocytic pockets are wide open (Chandler et al., 1989). This suggests that small molecular weight osmoticants specifically inhibit pore growth, possibly by halting granule matrix dispersal or by stiffening of the cortical cytoskeleton due to actin polymerization.

In conclusion, our results do not support a role for granule swelling as a prerequisite for granule-plasma membrane fusion. In fact, our observations indicate that granule shrinkage during hyperosmotic conditions is not sufficient to block granule-plasma membrane fusion if the granules are properly docked. This suggests that granule swelling prior to fusion is not a *sine qua non* for exocytosis. Rather, the dramatic effect of osmolality on the cortex appears to be operating by mechanisms different than prevention of granule swelling. Hyperosmolality blocks exocytosis in sea urchin eggs by formation of a GFZ that separates most cortical granules from the plasma membrane. This prevents approach of granule and plasma membrane prior to fusion. The few granules which remain docked do fuse, but widening of the exocytic pocket is arrested immediately after the initial pore forms.

We thank Dr. Ronald Alvarado for use of his osmometer and Michael Quinlan for assistance in preparing the graphs. This study was supported by grants from National Science Foundation (DCB-8810200) and from the National Institutes of Health (HD 00619) to D.E.C.

References

- Begg, D.A., Rebhun, L.I. 1979. pH regulates the polymerization of actin in the sea urchin egg cortex. *J. Cell Biol.* **83**:241–248
- Bilinski, M., Plattner, H., Matt, H. 1981. Secretory protein decondensation as a distinct, Ca²⁺-mediated event during the final stages of exocytosis in *Paramecium* cells. *J. Cell Biol.* **88**:179–188
- Breckenridge, L.J., Almers, W. 1987. Final steps in exocytosis in a cell with giant secretory granules. *Proc. Natl. Acad. Sci. USA* **84**:1945–1949
- Chandler, D.E., Bennett, J.P., Gomperts, B. 1983. Freeze-fragmentation studies of chemotactic peptide-induced exocytosis in neutrophils: Evidence for two patterns of secretory granule fusion. *J. Ultrastruct. Res.* **82**:221–232
- Chandler, D.E., Heuser, J.E. 1980. Arrest of membrane fusion events in mast cells by quick-freezing. *J. Cell Biol.* **86**:666–674
- Chandler, D.E., Whitaker, M., Zimmerberg, J. 1989. High molecular weight polymers block cortical granule exocytosis in sea urchin eggs at the level of granule matrix disassembly. *J. Cell Biol.* (in press)
- Cohen, F.S., Akabas, M.H., Zimmerberg, J., Finkelstein, A. 1984. Parameters affecting the fusion of unilamellar phospholipid vesicles with planar bilayer membranes. *J. Cell Biol.* **98**:1054–1062
- Cohen, F.S., Zimmerberg, Z., Finkelstein, A. 1980. Fusion of phospholipid vesicles with planar phospholipid bilayer membranes. II. Incorporation of a vesicular membrane marker into the planar membrane. *J. Gen. Physiol.* **75**:251–270
- Finkelstein, A., Zimmerberg, J., Cohen, F.S. 1986. Osmotic swelling of vesicles: Its role in the fusion of vesicles with planar phospholipid bilayer membranes and its possible role in exocytosis. *Annu. Rev. Physiol.* **48**:163–174
- Gilligan, D.M., Satir, B. 1983. Stimulation and inhibition in *Paramecium*: Role of divalent cations. *J. Cell Biol.* **97**:224–234
- Grinstein, S., Cohen, S., Goetz, J.D., Rothstein, A. 1985. Osmotic and phorbol ester-induced activation of Na⁺/H⁺ exchange: Possible role of protein phosphorylation in lymphocyte volume regulation. *J. Cell Biol.* **101**:269–276
- Hampton, R.Y., Holz, R.W. 1983. Effects of changes in osmolality on the stability and function of cultured chromaffin cells and the possible role of osmotic forces in exocytosis. *J. Cell Biol.* **96**:1082–1088
- Henson, J.H., Begg, D.A. 1988. Filamentous actin organization in the unfertilized sea urchin egg cortex. *Dev. Biol.* **127**:338–348
- Heuser, J.E., Reese, T.S., Dennis, M.J., Jan, Y., Jan, L., Evans, L. 1979. Synaptic vesicle exocytosis captured by quick freezing and correlated with quantal transmitter release. *J. Cell Biol.* **81**:275–300
- Holz, R.W. 1986. The role of osmotic forces in exocytosis from adrenal chromaffin cells. *Annu. Rev. Physiol.* **48**:175–189
- Kazilek, C.J., Merkle, C.J., Chandler, D.E. 1988. Hyperosmotic inhibition of calcium signals and exocytosis in rabbit neutrophils. *Am. J. Physiol.* **254**:C709–C718
- Mabuchi, I., Spudich, J.A. 1980. Purification and properties of soluble actin from sea urchin eggs. *J. Biochem.* **87**:785–802
- Parker, J.C., Castranova, V. 1984. Volume-responsive sodium and proton movements in dog red blood cells. *J. Gen. Physiol.* **84**:379–401
- Payan, P., Girard, J.P., Ciapa, B. 1983. Mechanisms regulating intracellular pH in sea urchin eggs. *Dev. Biol.* **100**:29–38
- Plattner, H., Reichel, K., Matt, H. 1977. Bivalent-cation-stimulated ATPase activity at preformed exocytosis sites in *Paramecium* coincides with membrane-intercalated particle aggregates. *Nature (London)* **267**:702–704
- Pollard, H.B., Pazoles, C.J., Creutz, C.E., Scott, J.H., Zinder, O., Hotchkiss, A. 1984. An osmotic mechanism for exocytosis from dissociated chromaffin cells. *J. Biol. Chem.* **259**:1114–1121
- Pollard, H.B., Tack-Goldman, K., Pazoles, C.J., Creutz, C.E., Shulman, N.R. 1977. Evidence for control of serotonin secretion in human platelets by hydroxyl ion transport and osmotic lysis. *Proc. Natl. Acad. Sci. USA* **74**:5295–5299
- Reynolds, E.S. 1963. The use of lead citrate at high pH as an electron-opaque stain in electron microscopy. *J. Cell Biol.* **17**:208–212
- Whitaker, M., Zimmerberg, J. 1987. Inhibition of secretory granule discharge during exocytosis in sea urchin eggs by polymer solutions. *J. Physiol. (London)* **389**:527–539
- Zimmerberg, J., Curran, M., Cohen, F.S., Brodwick, M. 1987. Simultaneous electrical and optical measurements show that membrane fusion precedes secretory granule swelling during exocytosis of beige mouse mast cells. *Proc. Natl. Acad. Sci. USA* **84**:1585–1589
- Zimmerberg, J., Sardet, C., Epel, D. 1985. Exocytosis of sea urchin egg cortical vesicles in vitro is retarded by hyperosmotic sucrose: Kinetics of fusion monitored by quantitative light-scattering microscopy. *J. Cell Biol.* **101**:2398–2410
- Zimmerberg, J., Whitaker, M. 1985. Irreversible swelling of secretory granules during exocytosis caused by calcium. *Nature (London)* **315**:581–584

Received 4 April 1989; revised 24 July 1989